3.2

ESTIMATING AIR-SEA ENERGY AND MOMENTUM EXCHANGES INSIDE TROPICAL CYCLONES USING THE FETCH- AND DURATION-LIMITED WAVE GROWTH PROPERTIES

Paul A. Hwang[1] and Yalin Fan[2]
[1]Remote Sensing Division, Naval Research Laboratory, Washington, DC, USA
[2]Oceanography Division, Naval Research Laboratory, Stennis Space Center, MS

1. INTRODUCTION

For wind-generated waves, the wind-wave triplets (reference wind speed U_{10}, significant wave height H_s, and frequency spectral peak wave period T_p) are intimately connected through the fetch- or duration-limited wave growth functions (e.g., Hasselmann et al. 1973; Donelan et al. 1985; Kahma and Calkoen 1994; Young 1999; Hwang and Wang 2004). The full set of the wind-wave triplets can be obtained knowing only one of the three variables combined with the fetch x_f (duration t_d) information using the fetch-limited (duration-limited) wave growth functions, which constitute a pair of dimensionless equations describing the growth of wave height and wave period as a function of fetch or duration. The frequency-integrated air-sea energy and momentum exchange rates E_t and M_t are functions of the wind-wave triplets and can be quantified with the wind-wave growth functions (Hwang and Sletten 2008; Hwang 2009; Hwang and Walsh 2016).

Previous studies have shown that wave development inside hurricanes follows essentially the same growth functions established for steady wind forcing conditions (Young 1988, 1998, 2006; Hwang 2016; Hwang and Walsh 2016). Here we present the analysis of wind-wave triplets collected inside Hurricanes Bonnie 1998 and Ivan 2004 at category 2 to 4 stages using the airborne scanning radar altimeter (SRA) combined with the NOAA HRD hurricane wind velocity product (Powell et al. 1996; Wright et al. 2001; Moon et al. 2003; Fan et al. 2009). The data yield the wind-wave triplets inside the hurricanes along several (between 6 and 11) transects radiating from the hurricane center.

Using the wind-wave triplets from the 4 hurricane scenes (Table 1), a parameterization model is formulated for the effective fetch and duration at any location inside a hurricane. The fetch and duration model is applied to the time series of 2D hurricane wind fields from post analysis to investigate the detailed temporal evolution of the wave field and the associated energy and momentum exchanges over the hurricane coverage area. The spatial distributions of energy and momentum exchanges show considerable asymmetry. Referenced to the hurricane heading, the exchanges on the right half plane of the hurricane are much stronger than those on the left half plane, the right-to-left ratio of about 2:1 to 3:1 is common.

2. HARMONIC ANALYSIS OF HURRICANE FETCH AND DURATION

The fetch- and duration-limited wave growth functions connect the wind-wave triplets (U_{10}, H_s, T_p). Many different formulas of growth functions have been reported in the literature, in this study we use the results obtained from least squares fitting of five field experiments conducted under quasi-steady and near-neutral stability conditions, collectively called BHDDB (Burling 1959; Hasselmann et al. 1973; Donelan et al. 1985; Dobson et al. 1989; Babanin and Soloviev 1998), as described in Hwang and Wang (2004):

$$\frac{H_s^2 g^2}{16U_{10}^4} = 6.19\times10^{-7}\left(\frac{x_f g}{U_{10}^2}\right)^{0.81}, \quad \frac{2\pi U_{10}}{T_p g} = 11.86\left(\frac{x_f g}{U_{10}^2}\right)^{-0.24}, \quad (1)$$

$$\frac{H_s^2 g^2}{16U_{10}^4} = 1.27\times10^{-8}\left(\frac{t_d g}{U_{10}}\right)^{1.06}, \quad \frac{2\pi U_{10}}{T_p g} = 2.94\left(\frac{t_d g}{U_{10}}\right)^{-0.34}, \quad (2)$$

where g is the gravitational acceleration (9.8 m/s^2). $H_s^2 g^2 / 16U_{10}^4 = \eta_{rms}^2 g^2 / U_{10}^4 = \eta_\#$ represents the wave energy $E = \rho_w g \eta_{rms}^2$, and $2\pi U_{10} / T_p g = U_{10} / c_p = \omega_\#$ is dimensionless frequency or inverse wave age; ρ_w is water density. The wind and wave measurements from the hurricane hunter missions provide the necessary data to calculate the effective fetches and durations for the locations where the wind and wave data are acquired (Hwang 2016; Hwang and Walsh 2016). Explicitly, the fetch and duration are derived by rearranging the variables in (1) and (2)

$$x_{\eta x} = 4.24\times10^7 U_{10}^{-2.93} H_s^{2.47}, \; x_{\omega x} = 2.29\times10^4 U_{10}^{-2.22} T_p^{4.22}, \quad (3)$$

$$t_{\eta t} = 1.75\times10^4 U_{10}^{-2.77} H_s^{3.77}, \; t_{\omega t} = 4.81\times10^4 U_{10}^{-2.22} T_p^{3.22}. \quad (4)$$

The analyses of Hwang (2016) and Hwang and Walsh (2016) show that x_f and t_d can be represented by linear functions of the radial distance r from the hurricane center:

$$x_{\eta x} = s_{\eta x}(\phi) r + I_{\eta x}(\phi), \; x_{\omega x} = s_{\omega x}(\phi) r + I_{\omega x}(\phi), \quad (5)$$

$$t_{\eta t} = s_{\eta t}(\phi) r + I_{\eta t}(\phi), \; t_{\omega t} = s_{\omega t}(\phi) r + I_{\omega t}(\phi), \quad (6)$$

where ϕ is the azimuth angle referenced to the hurricane heading, positive counterclockwise (CCW). The intercepts I and slopes s of the linear functions in (5) and (6) from processing the four hurricane scenes are shown in Fig. 1; these fitting parameters can be expressed in Fourier series:

$$q = a_0 + 2\sum_{n=1}^{N}\left(a_{n,q}\cos n\phi + b_{n,q}\sin n\phi\right), \quad (7)$$

where q can be $s_{\eta x}, I_{\eta x}, s_{\omega x}, I_{\omega x}, s_{\eta t}, I_{\eta t}, s_{\omega t}$ or $I_{\omega t}$. The curves computed with N=1, 2 and 3 are shown with continuous lines in Fig. 1; the data are well represented by (7) with N=3.

The harmonics a_{nq} and b_{nq} display a systematic quasi-linear variation with the radius of maximal wind speed r_m (Fig. 2)

$$Y = p_{1Y} r_m + p_{2Y}, \quad (8)$$

where Y represents $a_{n,q}$ and $b_{n,q}$ in (7). The fitting coefficients p_{1Y} and p_{2Y} are listed in Table 2 (the headers s_ex, I_ex, s_ox, I_ox, s_et, I_et, s_ot and I_ot represent $s_{\eta x}, I_{\eta x}, s_{\omega x}, I_{\omega x}, s_{\eta t}, I_{\eta t}, s_{\omega t}$ and $I_{\omega t}$.

3. DERIVATION OF WAVE PARAMETERS AND AIR-SEA EXCHANGES FROM HURRICANE WIND FIELD

As discussed in Hwang (2016) and Hwang and Walsh (2016), for wind generated waves, (U_{10}, H_s, T_p) are

connected by the growth functions and the full set can be computed knowing only one of the three, coupled with the fetch or duration input. At the present, the hurricane wind field is the most available product so we illustrate the computation of wave parameters and the derived quantities such as E_t and M_t from the wind input. Rewriting (1), the equations for H_s and T_p with U_{10} and fetch inputs are

$$H_{sw} = 8.10\times10^{-4} U_{10}^{1.19} x_{\eta x}^{0.405}, T_{pw} = 9.28\times10^{-2} U_{10}^{0.526} x_{\omega x}^{0.237} . \quad (9)$$

Similarly, for U_{10} and duration inputs (2),

$$H_{sw} = 1.55\times10^{-4} U_{10}^{1.47} t_{\eta t}^{0.531}, T_{pw} = 3.53\times10^{-2} U_{10}^{0.690} t_{\omega t}^{0.310} . \quad (10)$$

The subscript *w* is appended to the wave variables in (9) and (10) to emphasize that the wind-sea portion is obtained with the fetch-limited wave growth functions. The fetch and duration in those equations are computed from the harmonic model described in section 2. Once (U_{10}, H_s, T_p) are available, the $\omega_\#$, $\eta_\#$, M_t and E_t can be calculated (Hwang and Sletten 2008; Hwang and Walsh 2016):

$$\begin{aligned} E_t &= \alpha_E \rho_a U_{10}^3;\ \alpha_E = 0.20\omega_\#^{3.3}\eta_\# \\ M_t &= \alpha_M \rho_a U_{10}^2;\ \alpha_M = 0.40\omega_\#^{4.3}\eta_\# \end{aligned} . \quad (11)$$

where ρ_a is the air density. Fig. 3 shows an example (approximately the middle point of case I14, 00Z 15 Sep 2004) of using the HWind U_{10} to compute the wave parameters and air-sea exchange rates.

If a long time series of hurricane wind field is available, the corresponding temporal variation of the wave field and air-sea exchanges can also be computed. Fig. 4 presents an application applied to Hurricane Ivan 2004 (Fan et al. 2009), showing (a) the energy exchange integrated over the hurricane coverage area (here defined as the circle with a 250-km radius), (b) the relative energy exchange contributions of the left- and right half-planes, (c) the momentum exchange integrated over the hurricane coverage area, and (d) the relative momentum contributions of the left- and right half-planes. These results show the temporal evolution and the asymmetric spatial distributions of energy and momentum exchanges, the right-to-left ratio of 2:1 to 3:1 is common.

4. SUMMARY

The wave fields inside hurricanes behave similarly to those generated by steady fetch- or duration-limited wind forcing conditions (Young 1998; 2006; Hwang 2016; Hwang and Walsh 2016). The full set of the wind-wave triplets (U_{10}, H_s, T_p) can be calculated with the fetch- or duration-limited growth functions knowing only one of three variables and accompanied with the fetch or duration information. Using the U_{10}, H_s and T_p measured inside four different hurricane scenes, we present a fetch and duration model for any location inside a hurricane. The E_t and M_t of a wind wave system are functions of the wind-wave triplets, and can be calculated as well. The procedure is very useful for investigating the spatial distribution and temporal evolution of the air-sea interaction processes inside hurricanes.

References

Babanin, A.V., and Y. P. Soloviev, 1998: Field investigation of transformation of the wind wave frequency spectrum with fetch and the stage of development. *J. Phys. Oceanogr.*, 28, 563-576.

Black, P. G. et al., 2007: Air-sea exchange in hurricanes: Synthesis of observations from the coupled boundary layer air-sea transfer experiment. *Bulle. Am. Meteorol. Soc.*, **88**, 357-374.

Burling, R. W., 1959: The spectrum of waves at short fetches. *Dtsch. Hydrogr. Z*., **12**, 96-117.

Dobson, F., W. Perrie, and B. Toulany, 1989: On the deep-water fetch laws for wind-generated surface gravity waves. *Atmos.-Ocean*, **27**, 210-236.

Donelan, M. A., J. Hamilton, and W. H. Hui, 1985: Directional spectra of wind-generated waves, *Phil. Trans. Roy. Soc. Lond.*, **A315**, 509-562.

Fan, Y., I. Ginis, T. Hara, C. W. Wright, and E. J. Walsh, 2009: Numerical simulations and observations of surface wave fields under an extreme tropical cyclone. *J. Phys. Oceanogr.*, **39**, 2097-2116.

Hasselmann, K. et al., 1973: Measurements of wind-wave growth and swell decay during the Joint North Sea Wave Project (JONSWAP). *Deutsch. Hydrogr. Z.*, Suppl. **A8(12)**, 95pp.

Holthuijsen, L. H., M. D. Powell, and J. D. Pietrzak, 2012: Wind and waves in extreme hurricanes. *J. Geophys. Res.,* **117**, C09003.

Hwang, P. A., 2006: Duration- and fetch-limited growth functions of wind-generated waves parameterized with three different scaling wind velocities. *J. Geophys. Res*., **111**, C02005.

Hwang, P. A., 2016: Fetch- and duration-limited nature of surface wave growth inside tropical cyclones: With applications to air-sea exchange and remote sensing. *J. Phys. Oceanogr*., **46**, 41-56.

Hwang, P. A., and M. A. Sletten, 2008: Energy dissipation of wind-generated waves and whitecap coverage. *J. Geophys. Res*., **113**, C02012.

Hwang, P. A., and D. W. Wang, 2004: Field measurements of duration limited growth of wind-generated ocean surface waves at young stage of development. *J. Phys. Oceanogr.*, **34**, 2316-2326..

Hwang, P. A., and E. J. Walsh, 2016: Azimuthal and radial variation of wind-generated surface waves inside tropical cyclones. *J. Phys. Oceanogr*. (in press).

Janssen, P., 2004: *The Interaction of Ocean Waves and Wind*. Cambridge Univ. Press, Cambridge, UK, 300 pp.

Kahma, K. K., and C. J. Calkoen, 1994: Growth curve observations. In *Dynamics and modeling of ocean waves*, (eds.) G.J. Komen, L. Cavaleri, M. Donelan, K. Hasselmann, S. Hasselmann, and P.A.E.M. Janssen, Cambridge University Press, 74-182.

Komen, G. J., L. Cavaleri, M. Donelan, K. Hasselmann, S. Hasselmann, and P. A. E. M. Janssen (Eds.), 1994: *Dynamics and modeling of ocean waves.* Cambridge Univ. Press, Cambridge, UK, 532 pp.

Moon, I.-J., I. Ginis, T. Hara, H. L. Tolman, C. W. Wright, and E J. Walsh, 2003: Numerical simulation of sea surface directional wave spectra under hurricane wind forcing. *J. Phys. Oceanogr.*, **33**, 1680-1706.

Pierson, W. J., and L. Moskowitz, 1964: A proposed spectral form for full, developed wind seas based on the similarity theory of S.A. Kitaigorodskii. *J. Geophys. Res.*, **69**, 5181-5190.

Powell, M. D., S. H. Houston, and T. A. Reinhold, 1996: Hurricane Andrew's landfall in south Florida. Part I: Standardizing measurements for documentation of surface wind fields. *Wea. Forecasting*, **11**, 304–328.

Wright, C. W., E. J. Walsh, D. Vandemark, W. B. Krabill, A. W. Garcia, S. H. Houston, M. D. Powell, P. G. Black, and F. D. Marks, 2001: Hurricane directional wave spectrum spatial variation in the open ocean. *J. Phys. Oceanogr.*, **31**, 2472-2488.

Young, I. R., 1988: Parametric hurricane wave prediction model, *ASCE J. Waterway, Port, Coastal and Ocean Eng.,* **114**, 637-652.

Young, I. R., 1998: Observations of the spectra of hurricane generated waves. *Ocean Eng.,* **25**, 261-276.

Young, I. R., 1999: *Wind generated ocean waves.* Elsevier, Amsterdam, the Netherlands, 288 pp.

Young, I. R., 2006: Directional spectra of hurricane wind waves. *J. Geophys. Res.,* **111**, C08020.

Table 1. Some basic information of the four datasets, collected in hurricane Bonnie 1998 and Ivan 2004, used for the analysis in this paper.

File ID	**B24**	**I09**	**I12**	**I14**
Start time UTC	8/24/1998 20:29	9/9/2004 16:15	9/12/2004 10:39	9/14/2004 20:09
End time UTC	8/25/1998 1:44	9/9/2004 20:10	9/12/2004 15:41	9/14/2004 2:49
HRD U10 max (m/s)	44.4	59.4	55.4	61.6
rm (km)	74.0	13.0	17.0	42.0
V_a (m/s)	4.5	4.5	3.9	4.5
theta_a (degN)	13.0	62.0	69.0	25.0
SRA U10 min	1.4	1.8	0.8	1.2
SRA U10 max	45.7	74.0	59.9	69.6
SRA Hs min	4.4	1.6	2.9	3.6
SRA Hs max	10.9	12.7	12.0	13.1
SRA Tp min	8.0	5.8	8.2	8.9
SRA Tp max	13.3	15.2	13.8	14.4
# SRA spectra	233	376	456	600

Table 2. Linear fitting coefficients of fetch and duration harmonics as a function of radius of maximum winds $Y = p_{1Y} r_m + p_{2Y}$ (8), where *Y* represents $a_{n,q}$ and $b_{n,q}$ in (7); see text for further explanation.

q	s_ex	l_ex	s_ox	l_ox	s_et	l_et	s_ot	l_ot
a0,q								
p1	-1.40E-02	1.95E+00	-3.04E-02	3.22E+00	-7.88E-04	1.07E-01	-1.47E-03	1.60E-01
p2	1.57E+00	-3.54E+01	3.27E+00	-1.42E+02	9.04E-02	-2.42E+00	1.58E-01	-6.73E+00
a1,q								
p1	-1.02E-02	1.26E+00	-1.34E-02	1.09E+00	-5.17E-04	5.76E-02	-6.11E-04	4.81E-02
p2	5.10E-01	-4.77E+01	9.85E-01	-5.22E+01	2.39E-02	-2.23E+00	3.99E-02	-2.18E+00
b1,q								
p1	5.21E-03	-8.23E-01	-1.27E-02	1.16E+00	1.54E-04	-2.81E-02	-5.75E-04	5.30E-02
p2	-6.87E-02	3.02E+01	1.51E+00	-1.02E+02	5.25E-03	8.52E-01	6.90E-02	-4.50E+00
a2,q								
p1	5.55E-03	-4.11E-01	1.23E-02	-1.10E+00	3.22E-04	-2.31E-02	6.14E-04	-5.28E-02
p2	-4.79E-01	2.25E+01	-1.01E+00	6.93E+01	-2.63E-02	1.27E+00	-4.91E-02	3.24E+00
b2,q								
p1	-3.32E-03	-1.52E-01	-2.00E-02	1.51E+00	-2.88E-04	5.96E-03	-9.14E-04	6.68E-02
p2	2.11E-01	8.86E+00	1.26E+00	-9.80E+01	1.58E-02	-2.16E-01	5.43E-02	-4.14E+00
a3,q								
p1	6.44E-03	-5.32E-01	1.45E-02	-9.21E-01	3.19E-04	-2.61E-02	6.23E-04	-3.91E-02
p2	-3.29E-01	2.85E+01	-8.47E-01	5.45E+01	-1.52E-02	1.31E+00	-3.41E-02	2.18E+00
b3,q								
p1	1.91E-03	-2.28E-01	-5.70E-03	1.01E+00	1.09E-04	-9.53E-03	-1.37E-04	3.62E-02
p2	-2.25E-01	2.11E+01	1.80E-01	-4.71E+01	-1.06E-02	8.72E-01	3.06E-03	-1.68E+00

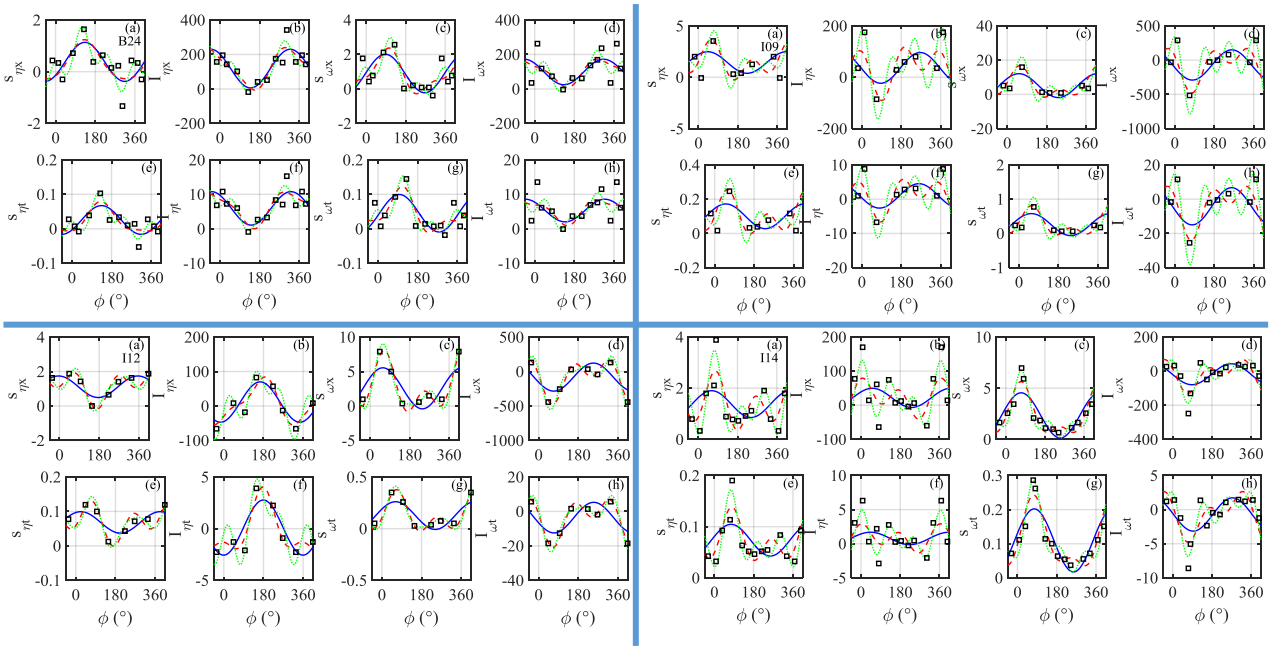

Fig. 1. Slope s_q and intercept I_q of $q = s_q(\phi) r + I_q(\phi)$, where q can be $x_{\eta x}, x_{\omega x}, t_{\eta t}$ or $t_{\omega t}$. The results obtained from datasets B24, I09, I12 and I14 (Table 1) are shown in the 4 quadrants, respectively upper left (UL), upper right (UR), lower left (LL) and lower right (LR). The solid, dashed and dotted curves corresponding to the first, second and third order Fourier series are also superimposed in each panel. For each dataset, s and I are plotted in (a) and (b) for $x_{\eta x}$, (c) and (d) for $x_{\omega x}$, (e) and (f) for $t_{\eta t}$, and (g) and (h) for $t_{\omega t}$.

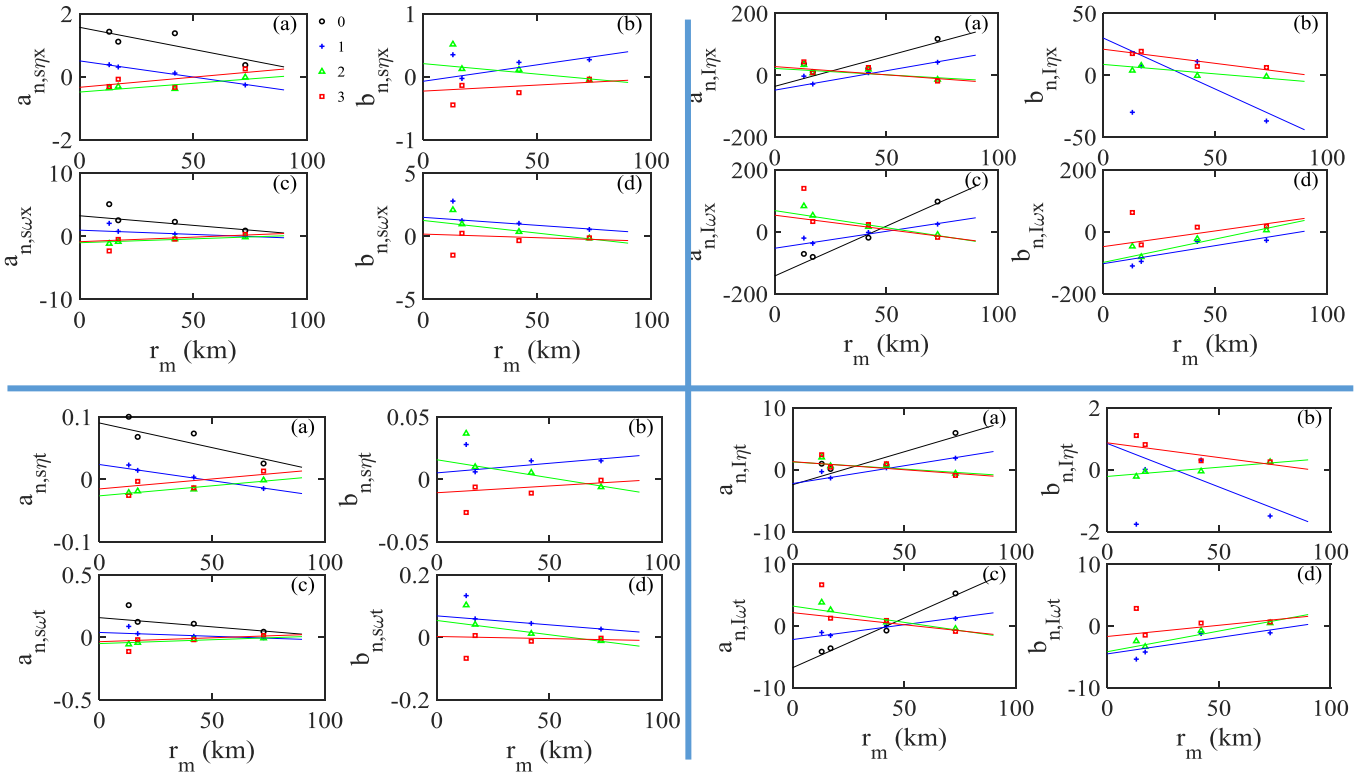

Fig. 2. Harmonic representations of the slopes and intercepts of the linear functions defining the fetch and duration, where q can be $s_{\eta x}, I_{\eta x}, s_{\omega x}, I_{\omega x}, s_{\eta t}, I_{\eta t}, s_{\omega t}$ or $I_{\omega t}$. The harmonics $a_{n,q}$ and $b_{n,q}$ show linear dependence on r_m, n=0, 1, 2, 3 ($b_{0,q}$=0). (UL): Slopes of fetch for wave height and wave period: (a) $a_{n,s_{\eta}x}$, (b) $b_{n,s_{\eta}x}$, (c) $a_{n,s_{\omega}x}$, and (d) $b_{n,s_{\omega}x}$; (UR): Intercepts of fetch for wave height and wave period: (a) $a_{n,I_{\eta}x}$, (b) $b_{n,I_{\eta}x}$, (c) $a_{n,I_{\omega}x}$, and (d) $b_{n,I_{\omega}x}$; (LL): Slopes of duration for wave height and wave period: (a) $a_{n,s_{\eta}t}$, (b) $b_{n,s_{\eta}t}$, (c) $a_{n,s_{\omega}t}$, and (d) $b_{n,s_{\omega}t}$; (LR): Intercepts of duration for wave height and wave period: (a) $a_{n,I_{\eta}t}$, (b) $b_{n,I_{\eta}t}$, (c) $a_{n,I_{\omega}t}$, and (d) $b_{n,I_{\omega}t}$.n.

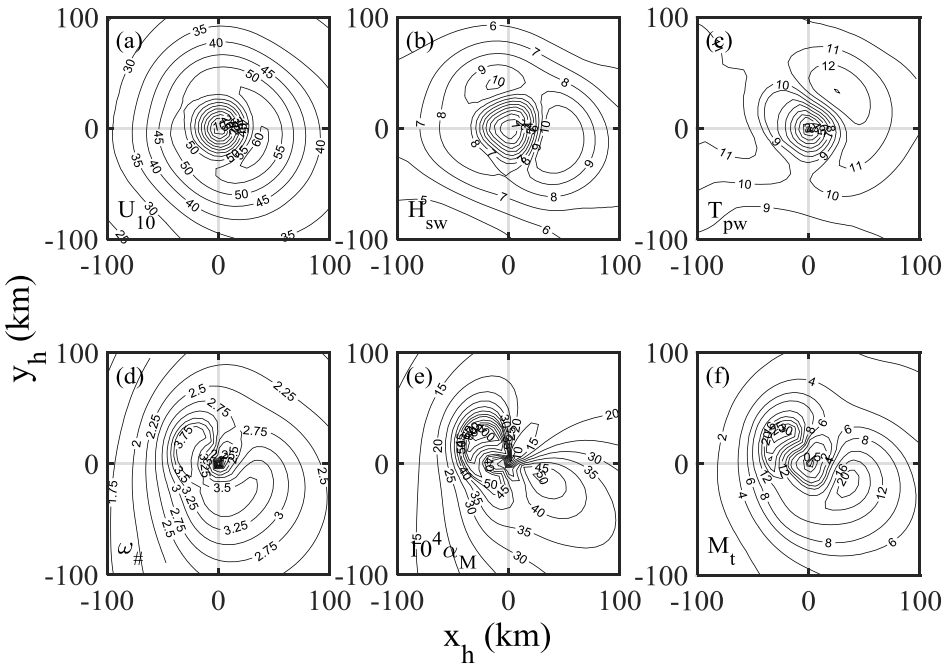

Fig. 3. An example illustrating the derivation of wave and air-sea interaction parameters using the hurricane wind field as an input, shown here are (a) input U_{10}, and outputs of (b) H_{sw}, (c) T_{pw}, (d) $\omega_\#$, (e) E_t, (f) M_t; subscript w emphasizes that the wave parameters derived from the fetch- and duration-growth functions are the wind sea components.

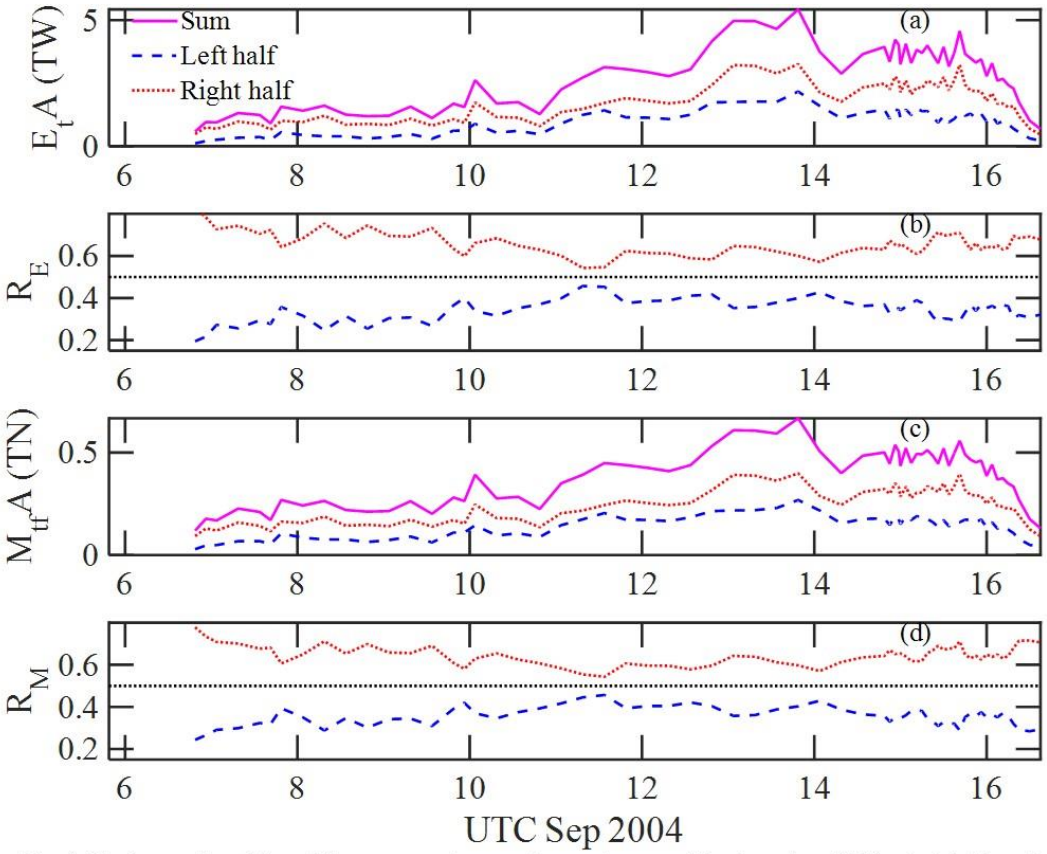

Fig. 4. The temporal evolution of the energy and momentum exchanges of Hurricane Ivan 2004 calculated from the time seried of the HWind time series from 06 to 17 Sep: (a) E_t integrated over the hurricane coverage area of 250-km radius, and the left and right half contributions; (b) the fractional E_t contributions of the left and right half planes, (c) M_t integrated over the hurricane coverage area of 250-km radius, and the left and right half contributions; and (d) the fractional M_t contributions of the left and right half planes.